Iranian Journal of Medical Physics

ijmp.mums.ac.ir

DTI-Derived Connectome and Deep Learning Approach for Differentiation of Alzheimer's Disease and Frontotemporal Dementia

Fatemeh Mohammadian[1], Ali Shoeibi[2], Sara Mirabian[3], Zohre Ganji[3], Hoda Zare[4*]

1. Department of Medical Physics and Radiology, Faculty of Paramedicine, Gonabad University of Medical Sciences, Gonabad, Iran
2. Department of Neurology, Faculty of Medicine, Mashhad University of Medical Sciences, Mashhad, Iran
3. Department of Medical Physics, Faculty of Medicine, Mashhad University of Medical Sciences, Mashhad, Iran
4. Medical Physics Research Center, Mashhad University of Medical Sciences, Mashhad, Iran

ARTICLE INFO

Article type:
Original Paper

Keywords:
Frontotemporal Dementia
Alzheimer's Disease
Magnetic Resonance Imaging
Diffusion Tensor Imaging
Deep Learning

ABSTRACT

Introduction: Frontotemporal dementia and Alzheimer's disease exhibit overlapping symptoms, making differential diagnosis challenging. While magnetic resonance imaging and diffusion tensor imaging provide valuable information about the structure of the brain, the integration of these data and applying a deep learning model for classifying frontotemporal dementia and Alzheimer's disease remains relatively unexplored. We aimed to construct structural connectomes using quantitative tractography and evaluate a deep learning model's performance in classifying Frontotemporal dementia, Alzheimer's disease, and normal individuals.

Material and Methods: Neuroimaging data from a total of 360 subjects, including patients with Frontotemporal dementia, Alzheimer's disease, and cognitively normal individuals. By merging T1-weighted and DTI scans, a structural connectivity matrix was constructed. To enable accurate diagnosis using those connectomes, we trained a Connectome-Inception Convolutional Neural Network. Model performance was assessed using five-fold stratified cross-validation, with data augmentation (SMOTE) applied exclusively to the training and validation folds.

Results: This approach recognized discriminative features of the brain across studied groups. Mean classification accuracy was 0.689 for ternary classification of Frontotemporal dementia/Alzheimer's disease/cognitively normal individuals, and 0.746, 0.721, and 0.767 for the binary classification of Frontotemporal dementia vs. Alzheimer's disease, Frontotemporal dementia vs. cognitively normal individuals, and Alzheimer's disease vs. cognitively normal individuals, respectively (AUC range: 0.826-0.869 for binary classification, 0.854 for the ternary classification).

Conclusion: The results suggest that structural connectome-based features can meaningfully discriminate between studied groups, potentially reflecting disease-vulnerable brain connections. These findings support structural connectomes as a promising and interpretable feature representation for differentiating these conditions, warranting further validation on independent, harmonized cohorts.

►*Please cite this article as:*
Mohammadian F, Shoeibi A, Mirabian S, Ganji Z , Zare H. DTI-Derived Connectome and Deep Learning Approach for Differentiation of Alzheimer's Disease and Frontotemporal Dementia. Iran J Med Phys 2026; 23 (3): 181-190. 10.22038/ijmp.2026.96453.2713.

Introduction

Frontotemporal dementia (FTD) is an early neurodegenerative syndrome and the third most common form of dementia, accounting for approximately 20% of all cases. It is one of the significant causes of dementia in individuals under 65 years old [1, 2]. The clinical manifestations of FTD include behavioral changes, executive function impairment, and language difficulties. However, due to the overlap of symptoms with other types of dementia and psychological disorders, diagnosing FTD presents challenges [1, 3]. In the early stage of FTD, mild atrophy is observed in the frontal and temporal lobes. At the second stage, atrophy spreads to other areas of the brain. At the third level, the deep white matter undergoes atrophy, and at the fourth level, severe atrophy occurs in the frontal and temporal lobes, leading to the disappearance of white matter [4]. Alzheimer's disease (AD), an age-related and the most prevalent type of neurodegenerative disease, occurs in 3% of individuals aged 65 to 74, 17% of the population aged 75-84, and 32% of individuals over 85 years old [5-7]. The primary symptom of AD is the loss of short-term memory followed by a decline in long-term memory. As the disease progresses, patients experience difficulties in motor tasks, sleep disorders, and finally, develop incontinence and complete dependence [8]. FTD and AD share many clinical symptoms, and cognitive impairments often lead to misdiagnosis [9]. There is no curative treatment for FTD and AD, and their differential

*Corresponding Author: Tel: +98- 38002321; Fax: +98-38002320; Email: zareh@mums.ac.ir

diagnosis is often difficult in the early stages, so 18.18% of individuals with AD are misdiagnosed and receive inappropriate medication, which affects disease-controlling procedures[10-12]. Differential diagnosis between these two diseases after observing the clinical symptoms of dementia is crucial to providing targeted treatment and care for patients.

Neuroimaging techniques have a major role in the clinical diagnosis of FTD and AD. Magnetic resonance imaging (MRI), positron emission tomography (PET), computed tomography scan (CT), and single photon emission computed tomography (SPECT) are commonly used as imaging modalities [13-15]. Among these, MRI plays an essential role in the diagnosis of structural and functional brain alterations and related biomarkers in FTD and AD [15].

Advanced MRI modalities like diffusion tensor imaging (DTI) potentially provide characteristic signs of every neurodegenerative disorder and can be helpful for diagnostic procedures [15, 16]. DTI measures the translational motion of water molecules and their anisotropy in the brain. In neurological diseases, DTI can detect variations in white matter fiber pathways compared to a healthy brain [17]. Fractional anisotropy (FA), which measures the fraction of anisotropic diffusion and is extracted from DTI images, is the most widely used scale to determine the integrity of brain white matter [18].

The human brain has a complex system, and the identification of its anatomical connections can play a crucial role in better understanding the relationship between brain functional defects and structural disruption in individuals with brain disorders [19, 20]. Using DTI images makes it possible to determine the orientation of white matter fibers and especially, utilizing probabilistic tractography has been developed to investigate the anatomical connections of the brain [21]. Tractography is a technique used to sample the orientation of fibers and determine fiber directions. An inherent limitation of simple tractography is the unknown exact time of termination of the fiber direction, which may reduce the accuracy of reconstructed connections [22]. Construction of a structural connectome using FA biomarker determines how brain regions are connected based on FA and can be advantageous in differential diagnosis of FTD and AD.

Machine learning (ML) is a set of statistical algorithms designed to perform various tasks, such as prediction, automatically [23]. These algorithms take the input data and generate the desired outputs through computational processes [24]. As a subset of machine learning, deep learning (DL) is a technique that employs multiple nonlinear processing layers to identify complex high-dimensional patterns [25]. Various types of deep learning models are proposed to perform different tasks, and the most common ones are diverse types of artificial neural networks that focus on feature learning [26]. Artificial neural network models are rapidly developing, and one of the most well-known models is the convolutional neural network (CNN), which is generally an interesting deep learning model in medical imaging and a powerful method for training models with image features and other structured data [27]. One of these models is the Connectome-Inception Convolutional Neural Network (ConCeptCNN) proposed in 2022 by Ming Chen [28], which measures the variance of brain regions' connections in neurological disease and extracts multi-scale topological features from brain connectomes. Compared with other CNN-based approaches, ConCeptCNN improves feature extraction performance by using multiple vector-shaped convolutional filters, allowing the model to obtain complementary topological information from brain connectome data at different levels [28]. Figure 2 shows the schematic representation of the model.

However, prior studies have explored the differential diagnosis of FTD and AD using machine learning algorithms and different MRI modalities [29-34]. Möller et al. [29] and Kim et al. [30] applied machine learning for FTD/AD differentiation and have largely relied on traditional machine learning applied to structural MRI features. Bron et al. [31] and Bouts et al. [32] analyzed DTI-derived measures without connectome-level integration. In addition, deep learning architectures originally designed for natural images or voxel-wise MRI data, rather than for the topological structure of brain connectomes in Ma et al. [33], and Hu et al. [34] studies. As a result, the specific structural connectivity pattern linking distributed brain regions, which may carry diagnostically relevant information beyond regional atrophy or voxel-wise signal changes, remains comparatively underexplored for this differential diagnosis, particularly in a ternary classification of FTD, AD, and cognitively normal (CN) controls. The present study addresses this gap by combining structural connectomes constructed via anatomically constrained tractography (ACT) and FA with ConCeptCNN. To our knowledge, this combination, ACT/FA-derived structural connectomes analysed using a connectome-specific multi-scale CNN architecture for binary and ternary classification of FTD, AD, and CN has not been previously reported. Eventually, the diagnostic performance and robustness of the ConCeptCNN architecture were evaluated for both binary and three-way classification among the three studied groups.

Materials and Methods

Data acquisition

In this study, neuroimages in structural MRI and DTI modalities in the FTD, AD, and CN subjects were obtained from the Neuroimaging Institute of Frontotemporal Degeneration (NIFD) database and the Alzheimer's Disease Neuroimaging Initiative (ADNI) database. Diagnostic classification was based on the established clinical assessment procedures of the respective source databases. In the NIFD, participants

with frontotemporal dementia were established through comprehensive clinical assessments, including physician interviews and neurological examination, cognitive and neuropsychological testing, informant interviews, and brain MRI. Cognitively normal NIFD participants were assessed as clinically and cognitively unimpaired through the same comprehensive evaluation framework. For the ADNI, AD classification was based on standardized clinical and cognitive assessments conducted according to the ADNI study protocol. The diagnostic assessment incorporated clinical evaluation and cognitive testing, including measures of global cognition, memory, and functional status. CN participants were classified based on the absence of significant cognitive impairment according to the ADNI clinical framework. Detailed information regarding the cohort composition, diagnostic classification, clinical assessments, and biomarker collection is provided in the official ADNI and NIFD study documentation[35, 36].

Ethical considerations

The presented study adheres to the Declaration of Helsinki of the World Medical Association, revised in 2013 for experiments involving humans. This article is taken from the MSc thesis and involves human participants that were reviewed and approved by the [Research Ethics Committee of the School of Medicine-Mashhad University of Medical Sciences] with ethics code: IR.MUMS.MEDICAL.REC.1401.263. Since pre-prepared data was used, there is no need for a consent statement.

In general, we analyzed the structural MRI and DTI data of 360 individuals, including 120 subjects with FTD, 120 subjects with AD, and 120 subjects in the control group. All data were labeled according to the classification of the NIFD and ADNI databases. Table 1 illustrates demographic information on the subjects. Images were obtained from GE and SIEMENS scanners with a field strength of 3 Tesla. The structural images were T1-weighted with MPRAGE and IRSPGR sequences, while the diffusion images were obtained in all three groups with b=2000 and b=1000 s/mm^2, slice thickness of 2 mm, Echo-Planar (EP) imaging sequence, and 64 and 48 gradient directions. No explicit cross-protocol harmonization was applied to reconcile these acquisition differences, which is addressed as a limitation in the discussion.

Table 1. Demographic data. The demographic information of individuals with FTD, AD, and NC groups.

	FTD	AD	CN
Number	120	120	120
gender (F/m)	59/61	44/76	67/53
Age	64.23 ± 7.53	75.41 ± 7.86	64.48 ± 9.56
Data Source	NIFD	ADNI	NIFD / ADNI

Preprocessing

The raw data obtained from the NIFD and ADNI databases may contain noise, artifacts, or distortions that could affect tractography. Therefore, it is necessary to pre-process data to construct appropriate structural connectomes. Structural and DTI images are processed in two different ways and are merged after registration.

Firstly, motion correction, non-uniformity intensity normalization, and skull stripping were performed on T1 images using the Freesurfer software (version 7.3.2) [37]. The T1-weighted images of each subject's cerebral cortex were parcellated into 84 regions using Freesurfer software and Desikan-Killiany-Tourville (DKT) atlas [38]. These parcellated images are utilized as a reference for nodes of the structural connectome network.

Preprocessing of diffusion images was performed using MRtrix3 (version 3.0.3) [39], including noise reduction using “dwidenoise” command, motion and eddy current correction, and correction for susceptibility-induced distortion arising from differences in magnetic sensitivity between tissue types using “dwipreproc” command, following visual inspection for quality control.

Tractography

Anatomical constrained tractography (ACT) was used for fiber pathway reconstruction, with seeding performed at the white matter (WM)/gray matter (GM) interface rather than throughout the WM, to improve the uniformity of fiber density.

To enhance the accuracy of tractography and utilize the information of structural images, T1 and diffusion images were registered. This was performed using the “epi_reg” command in FSL (version 6.0.5.2). After registration, a brain mask was created, and the fiber orientation distribution (FOD) was estimated using constrained spherical deconvolution (CSD) via the Tournier algorithm [40], improving the robustness of spherical deconvolution and the separation of fiber population at small crossing angles [41]. Whole-brain streamlines were constructed based on ACT with one million tracks, a maximum fiber length of 250 mm, a maximum curvature angle of 90 °, and a step size of 0.5mm, constrained fiber pathways using 5-tissue-type (5tt) and GM / WM interface maps. The brain is subdivided into 5 tissue types including cerebrospinal fluid (CSF), WM, cortical GM, subcortical GM, and pathological tissue, to identify GM / WM interfaces [22]. To make the density of streamlines proportional to the fiber density, the spherical deconvolution-informed filtering of tractograms (SIFT) was applied; SIFT improves the correspondence between streamline density and fiber orientation information, though it does not guarantee complete removal of false-positive pathways or resolve all sources of tractography bias[42].

Structural connectome

The structural connectivity matrix, also known as the structural connectome, is a network of connections between brain regions (nodes) defined in an N*N matrix [43]. The quantitative information of fiber pathways is stored in the connectivity matrix, and the fiber tracts are counted in each tractogram. The connectivity matrix with 84*84 dimensions was obtained using the DKT atlas, which divides the brain into 84 regions. Data processing steps to generate a structural connectome are summarized in Figure 1.

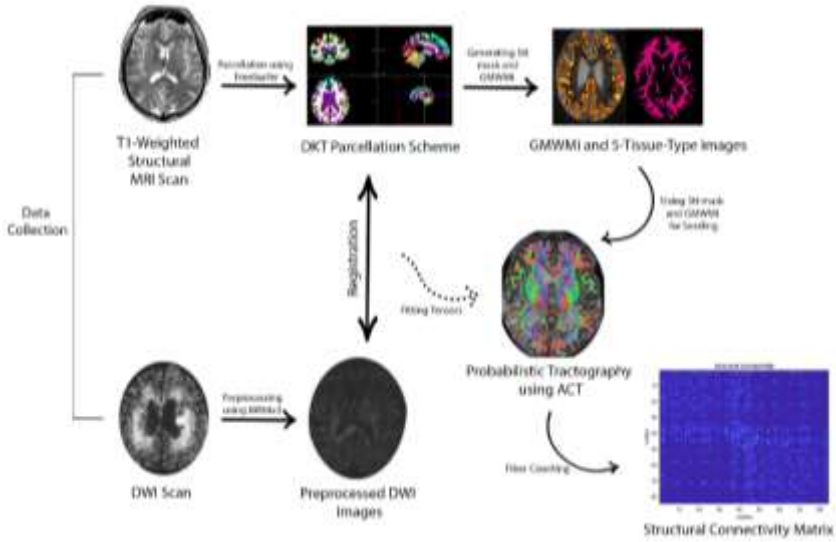


Figure 1. Image processing steps. The DWI and T1-weighted scans were processed to generate the final output, which is the connectivity matrix.

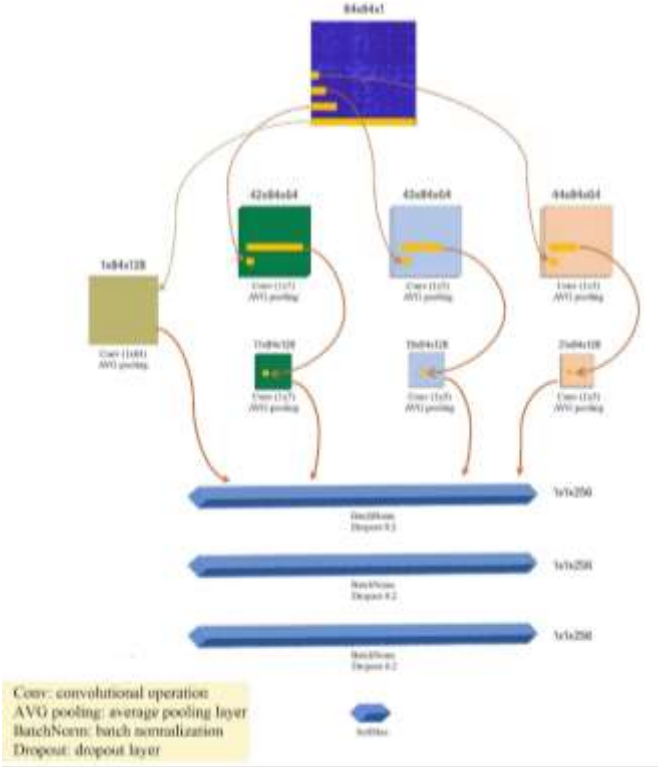


Figure 2. The schematic representation of ConCept CNN. Modified ConCept CNN comprises four channels with different filter dimensions convolved with the connectivity matrix as network input. Eventually, the outputs of channels are concatenated and given to fully connected layers to calculate class-membership probability.

Connectome augmentation

To enhance the performance of the deep learning neural network model, it is essential to have sufficient data available to prevent underfitting. In addition, the complex nature of the deep learning neural network model and the large number of learning parameters may cause overfitting if the number of subjects is not enough. In this study, the dataset consisting of 360 subjects is relatively small for training the model. To avoid data leakage between training and test data, the dataset was first partitioned into training, validation, and test subtests using five-fold stratified cross-validation, ensuring that each subject was assigned to the held-out test fold exactly once across the five folds. Only after the partitioning was the Synthetic Minority Over-sampling Technique (SMOTE) applied to generate synthetic connectomes, and it was applied exclusively to the training and validation subsets within each fold; the test subset in each fold remained entirely unaugmented and unseen during the training.

Deep learning model architecture

Considering that the input data to the neural network is a connectivity matrix, we employed the ConCeptCNN to better extract hidden features of structural connectomes.

ConCeptCNN architecture consists of four developed CNN-based channels, each using vector-shaped filters of a different scale: 1×3 (coarse_channel), 1×5 (medium_channel), 1×7 (fine_channel), and 1×84 (global_channel). The coarse, medium, and fine channels each contain two convolutional layers, with a pooling layer following each. The output of all four channels are concatenated and passed to a global average pooling layer, followed by three fully connected (dense) layers. The final layer uses a SoftMax (ternary classification) or sigmoid (binary classification) activation to compute class membership probabilities. Figure 3 illustrates the schematic representation and architecture of the modified ConCept CNN model.

Relative to the original ConCeptCNN architecture proposed by Chen et al. [28], this study made two modifications to reduce overfitting given the relatively limited sample size relative to model capacity; (1) the final flattening operation preceding the dense layers was replaced with global average pooling, substantially reducing the number of trainable parameters in the first dense layer; and (2) dropout regularization with the rate = 0.5 for binary classification and 0.2 for the three-class classification and L2 weight regularization ($\lambda = 0.001$) were applied to the fully connected layers.

Hyperparameter Settings

Model optimization was performed using Adam optimization with a learning rate of 0.0001. For binary classification, the binary cross-entropy loss function was used, and for ternary classification, the categorical cross-entropy loss function was used. All models were trained with a batch size of 16, for up to 100 epochs, with early stopping (patience = 15 epochs, monitoring validation loss, restoring the best-performing weights) to prevent unnecessary overfitting and ensure convergence.

All modifications of ConCeptCNN were implemented using the TensorFlow (version 2.10.0) and Keras (version 2.10.0) frameworks, along with Pandas (version 2.3.3), NumPy (version 1.26.4), and scikit-learn (version 1.6.1) libraries. All image processing was performed on Linux Ubuntu 20.04, and processing related to the ConCeptCNN was performed on Windows 10 with an NVIDIA GeForce RTX 2060 graphics processor (6 GB of dedicated memory) with a 64-bit Intel i7 central processing unit (CPU).

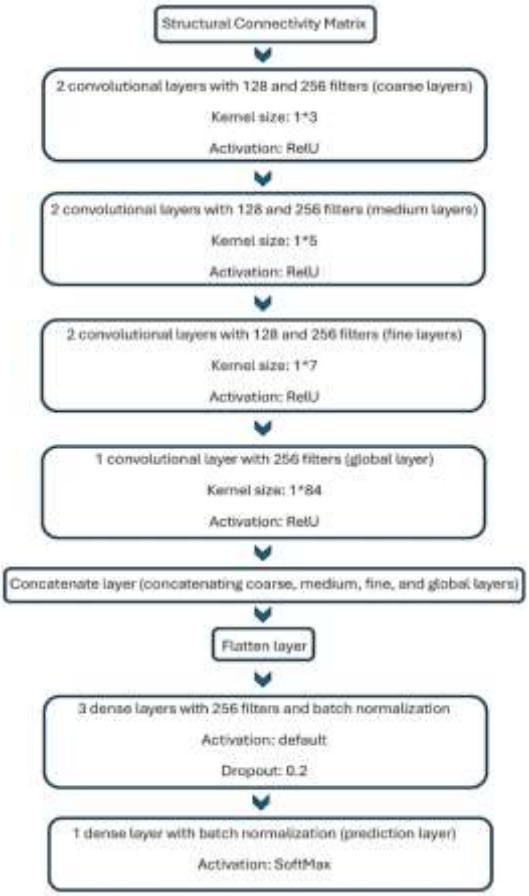


Figure 3. Architecture of modified ConCeptCNN layers. The order and detail of layers in the ConCept CNN architecture, including convolutional layers, concentrate layers, and dense layers

Performance evaluation metrics

Model performance was evaluated using accuracy, sensitivity (recall), specificity, precision, F1-score, and the area under the receiver operating characteristic curve (AUC). For the three-class (FTD/AD/CN) classification, sensitivity, specificity, precision, and F1-score were computed per class and then macro-averaged (i.e., averaged across classes without weighting by class size). The AUC was computed using a one-vs-rest approach, averaged across the three classes. Receiver operating characteristics (ROC) curves were plotted for each binary classification task to visually illustrate the trade-off between sensitivity and specificity across classification thresholds.

Results

The performance of ConCeptCNN was evaluated for the ternary classification of FTD, AD, and CN, as well as the three binary classifications (FTD/AD, FTD/CN, and AD/CN), using FA biomarker and DKT atlas-based structural connectome. All results reported in this section are derived from five-fold stratified cross validation, in which the dataset was partitioned into training, validation, and test subsets prior to any data augmentation. Reported values represent the mean and standard deviation of each metric across five folds.

Training and validation accuracy and loss curves for the ConCeptCNN model, for both the ternary and binary classification tasks, are presented in Figure 4, illustrating model convergence behavior across training epochs. Confusion matrices summarizing the pooled prediction across all cross-validation folds are presented in Figure 5 for each of the three binary classification tasks and the ternary classification task. The findings of the model evaluation are reported in Table 2.

For the ternary classification of FTD, AD, and CN, the model achieved a mean accuracy of 0.689 ± 0.051, sensitivity of 0.689 ± 0.051, specificity of 0.844 ± 0.025, precision of 0.722 ± 0.034, F1-score of 0.684 ± 0.049, and AUC of 0.854 ± 0.043 (macro-averaged across classes). The corresponding confusion matrix (Figure 5) shows the distribution of correct and incorrect classification across the three groups.

Among the binary classifications, the AD/CN task achieved the highest performance, with a mean accuracy of 0.767 ± 0.056, sensitivity of 0.817 ± 0.134, specificity of 0.717 ± 0.175, precision of 0.762 ± 0.106, F1-score of 0.777 ± 0.053, and AUC of 0.869 ± 0.049. The FTD/AD classification achieved a mean accuracy of 0.746 ± 0.142, sensitivity of 0.783 ± 0.170, specificity of 0.708 ± 0.401, precision of 0.799 ± 0.173, F1-score of 0.762 ± 0.080, and AUC of 0.860 ± 0.040. The FTD/ CN classification achieved a mean accuracy of 0.721 ± 0.079, sensitivity of 0.733 ± 0.277, specificity of 0.708 ± 0.283, precision of 0.768 ± 0.131, F1-score of 0.705 ± 0.135, and AUC of 0.826 ± 0.066. Confusion matrices for each binary task are shown alongside the ternary confusion matrix in Fig. 5, and the corresponding ROC curves, with AUC values for each binary comparison, are shown in Figure 6.

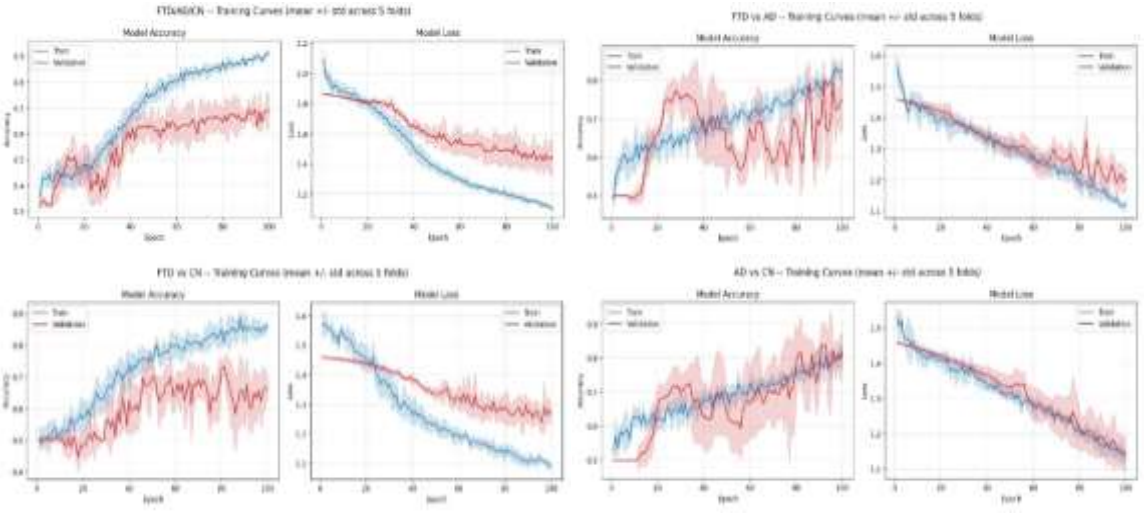


Figure 4. Loss function performances. A) The model accuracy and loss during training for binary and ternary classification.

Table 2. The findings of the proposed model performance evaluation for differentiating participants with FTD, AD, and CN groups.

	Mean Accuracy	Mean Sensitivity	Mean Specificity	Mean Precision	Mean F1-Score	Mean AUC
FTD/AD/CN	0.6889 ± 0.0507	0.6889 ± 0.0507	0.8444 ± 0.0253	0.7223 ± 0.0341	0.6843 ± 0.0492	0.8541 ± 0.0427
FTD/AD	0.7458 ± 0.1416	0.7833 ± 0.1703	0.7083 ± 0.4007	0.7987 ± 0.1731	0.7618 ± 0.0803	0.8597v ± 0.0402
FTD/CN	0.7208 ± 0.0788	0.7333 ± 0.2773	0.7083 ± 0.2826	0.7676 ± 0.1309	0.7051 ± 0.1346	0.8264 ± 0.0663
AD/CN	0.7667 ± 0.0559	0.8167 ± 0.1337	0.7167 ± 0.1753	0.7622 ± 0.1056	0.7765 ± 0.0532	0.8691 ± 0.0494

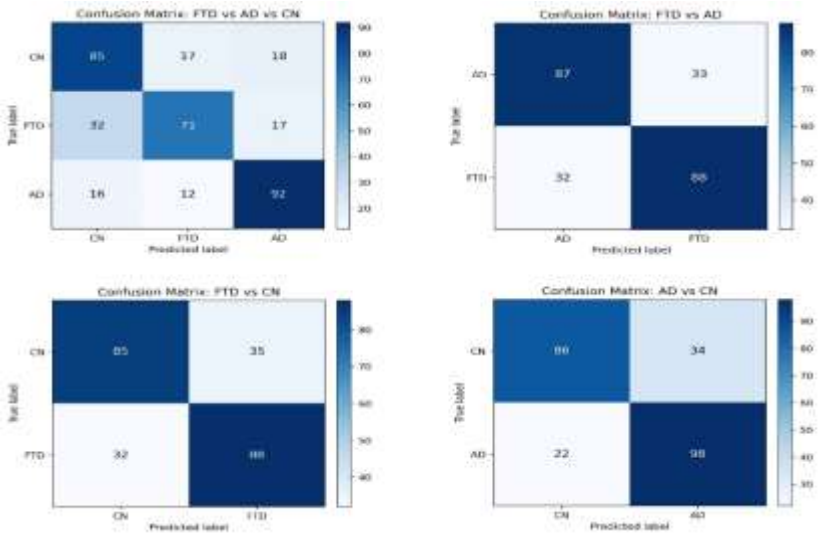


Figure 5. Confusion Matrices. Confusion matrices of the predictions across all cross-validation folds for ternary and binary classification tasks.

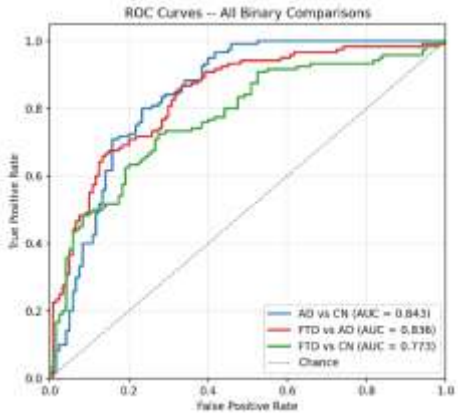


Figure 6. ROC curves. ROC curves based on AUC in binary classification tasks, including AD/CN (blue), FTD/AD (red), and FTD/CN (green).

Across all four classification tasks, AUC values ranged from 0.826 to 0.869, indicating that the model's underlying class separability was broadly consistent across comparisons, even where accuracy varied somewhat more between tasks. Consistent with the expectation that distinguishing among three overlapping neurodegenerative and control groups simultaneously is inherently more difficult than a pairwise distinction, ternary classification accuracy (0.689) was lower than each of the three binary classification accuracy (0.721-0.767).

Taken together, these results indicate that features derived from FA-based structural connectomes, processed through ConCeptCNN, carry discriminative information relevant to differentiating FTD, AD, and CN groups, both individually and jointly. As no directly controlled comparison against alternative deep learning architectures or traditional machine learning methods was performed using the same dataset, preprocessing pipeline, and evaluation protocol in this study, these findings should be interpreted as evidence supporting the feasibility of this connectome-based approach rather than as a demonstration of superiority over prior methods.

Discussion

This study was conducted to classify patients with frontotemporal dementia, Alzheimer's, and healthy individuals efficiently using DTI-derived structural connectomes and a novel deep learning model called ConCeptCNN.

Generally, previous studies utilizing classical machine learning methods had troubles, such as small sample sizes and manual feature extraction. On the other hand, studies that employed deep learning methods for identifying FTD, AD, and healthy individuals focused on the application of structural and raw MRI data. In the present study, to overcome these issues, we used structural and diffusion MRI to construct brain structural connectomes as input to our modified ConCept convolutional neural network. Also, we employed the average FA biomarker as an intra-voxel marker for tractography and structural connectomes construction, which is more efficient in classifying individuals with different stages of Alzheimer's disease compared to other markers extracted from DTI data, as indicated by Kolahkaj's study [10].

One of the highlights of our work is the application of probabilistic tractography based on CSD combined

with ACT constraints, which we use to construct reliable structural connectomes for classifying participants with FTD, AD, and healthy individuals. This approach yielded that the utilization of ACT tractography, which uses anatomical information in the structural MRI images as a biological constraint, restricts the tracts only to the white matter, and ensures accurate termination of the fiber pathways. Employment of ACT-based tractograms to construct reliable structural connectomes, which included topological features in lower dimensionality, enables a comparatively lighter neural network architecture. Our results indicate that the structural brain connections derived from ACT/CSD-based tractography using the FA biomarker carry discriminative information relevant to differentiating patients with FTD, AD, and healthy individuals within the dataset. However, we note that this reflects classification performance under the retrospective, cross-validated condition of this study rather than a demonstration of clinical diagnostic utility, which would require prospective validation in a clinical setting. To our knowledge, this is among the first studies to employ CSD-based ACT tractography together with connectome-specific convolutional architecture (ConCeptCNN) for the three group classifications. We note this reflects the literature reviewed for this study rather than systematic research. Previous studies have used the combination of structural images with DTI images [31, 32], but, to our knowledge, have not used ACT or CSD tractography for this purpose.

Considering issues with the classification of FTD, AD, and CN individuals in previous studies, the ternary classification of these groups achieved reasonable accuracy in the current study. This may be due to the potential extraction of topological features from structural connectomes by ConCeptCNN, which is a dedicated network for connectomes. The DTI-derived brain structural connections and connectome-based deep neural network models were the principal contributors to discriminating individuals in our study, though we cannot directly attribute performance gains over prior approaches without a controlled comparison under identical dataset, preprocessing, and evaluation conditions, which was beyond the scope of this study.

Several limitations should be considered when interpreting these findings. First, the sample size (360 subjects across three groups) is relatively modest for training a deep learning model, which may limit the stability and generalizability of the learned features despite the use of cross-validation and regularization to mitigate overfitting. We attempted to use all appropriate DTI and structural data provided by the NIFD and ADNI databases, but the sample size was modest for training and evaluating the deep learning models. Second, the AD group was on average older than the FTD and control groups, consistent with the typical age of onset for each disease [2, 5-7]. Although this reflects the natural clinical presentation of these disorders, we cannot fully exclude the possibility that age-related structural changes contributed in part to the classification performance alongside disease-specific connectivity alterations. Third, as with most deep neural network models, ConCeptCNN functions largely as a black box, and the specific structural connections driving its classifications are not directly interpretable from the model itself, limiting mechanistic insight into which connectome features are most disease relevant. Fourth, the FTD subjects were drawn from the NIFD database, the AD subjects were drawn exclusively from ADNI, and the CN group comprised a mixture of subjects from both databases. These databases were acquired using different scanners (GE and SIEMENS) and diffusion protocols (different b-values and gradient direction counts), and no explicit harmonization procedure was applied. Because the CN group includes NIFD-acquired and ADNI-acquired data, this partially mitigates scanner-related confounds for the FTD/CN and AD/CN comparisons specifically, but the FTD/AD comparison remains more susceptible to this confound, and the model may be capturing scanner-related or protocol-related variance rather than purely disease-related structural differences. Finally, this study did not include validation on an independent, external cohort or a leave-site-out evaluation; consequently, the generalizability of these findings to independent and multi-site clinical populations remained uncertain, and performance may differ when the model is applied to data acquired under scanning protocols or clinical settings not represented in this dataset. Further work incorporating data harmonization techniques, external multi-site validation, and model interpretability analyses with age-matched subgroups would help clarify the extent to which the reported performance reflects generalizable, disease-related structural differences.

Conclusion

This study demonstrates that the topological features extracted from DTI-derived structural connectomes, combined with a connectome-specific deep learning architecture (ConCeptCNN), can distinguish between frontotemporal dementia, Alzheimer's disease, and cognitively normal individuals, both in three-class classification and in each pairwise comparison, within this retrospective dataset. These findings suggest that structural connectivity patterns may carry information relevant to differentiating these conditions, though this reflects classification performance under the specific conditions evaluated here rather than a demonstrated capability to detect connectivity alterations across neurodegenerative disorders more broadly.

Single-study nature of this work and the absence of external or prospective validation, these results should be regarded as an early step rather than evidence of clinical readiness. With further validation or independent, multi-site cohorts, this connectome-based approach may eventually be useful as a potential supporting tool alongside clinical assessment and other diagnostic measures.

Acknowledgment

The authors would like to thank the Vice-Chancellor of the Research Department at Mashhad University of Medical Sciences for supporting this project.

References

1. Bang J, Spina S, Miller BL. Frontotemporal dementia. Lancet. 2015;386(10004):1672-82.
2. Ratnavalli E, Brayne C, Dawson K, Hodges JR. The prevalence of frontotemporal dementia. Neurology. 2002;58(11):1615-21.
3. Vieira RT, Caixeta L, Machado S, Silva AC, Nardi AE, Arias-Carrión O, et al. Epidemiology of early-onset dementia: a review of the literature. Clin Pract Epidemiol Ment Health. 2013;9:88-95.
4. Kril JJ, Halliday GM. Pathological staging of frontotemporal lobar degeneration. J Mol Neurosci. 2011;45(3):379-83.
5. 2020 Alzheimer's disease facts and figures. Alzheimer's & Dementia. 2020;16(3):391-460.
6. Sisodia SS. Alzheimer's disease: perspectives for the new millennium. J Clin Invest. 1999;104(9):1169-70.
7. Bigham B, Zamanpour SA, Zare H. Features of the superficial white matter as biomarkers for the detection of Alzheimer's disease and mild cognitive impairment: A diffusion tensor imaging study. Heliyon. 2022;8(1):e08725.
8. Kumar A, Sidhu J, Goyal A, Tsao JW. Alzheimer disease. 2018.
9. Forman MS, Farmer J, Johnson JK, Clark CM, Arnold SE, Coslett HB, et al. Frontotemporal dementia: clinicopathological correlations. Ann Neurol. 2006;59(6):952-62.
10. Kolahkaj S, Zare H. A connectome-based deep learning approach for Early MCI and MCI detection using structural brain networks. Neuroscience Informatics. 2023;3(1):100118.
11. Yu Q, Mai Y, Ruan Y, Luo Y, Zhao L, Fang W, et al. An MRI-based strategy for differentiation of frontotemporal dementia and Alzheimer's disease. Alzheimers Res Ther. 2021;13(1):23.
12. Gaugler JE, Ascher-Svanum H, Roth DL, Fafowora T, Siderowf A, Beach TG. Characteristics of patients misdiagnosed with Alzheimer's disease and their medication use: an analysis of the NACC-UDS database. BMC Geriatr. 2013;13:137.
13. Khachaturian ZS. Diagnosis of Alzheimer's disease. Arch Neurol. 1985;42(11):1097-105.
14. McKhann GM, Albert MS, Grossman M, Miller B, Dickson D, Trojanowski JQ. Clinical and pathological diagnosis of frontotemporal dementia: report of the Work Group on Frontotemporal Dementia and Pick's Disease. Arch Neurol. 2001;58(11):1803-9.
15. Agosta F, Galantucci S, Filippi M. Advanced magnetic resonance imaging of neurodegenerative diseases. Neurological Sciences. 2017;38(1):41-51.
16. Bigham B, Zamanpour SA, Zemorshidi F, Boroumand F, Zare H, for the Alzheimer′s Disease Neuroimaging I. Identification of Superficial White Matter Abnormalities in Alzheimer′s Disease and Mild Cognitive Impairment Using Diffusion Tensor Imaging. Journal of Alzheimer's Disease Reports. 2020;4:49-59.
17. Lope-Piedrafita S. Diffusion Tensor Imaging (DTI). Methods Mol Biol. 2018;1718:103-16.
18. O'Donnell LJ, Westin CF. An introduction to diffusion tensor image analysis. Neurosurg Clin N Am. 2011;22(2):185-96, viii.
19. Sporns O, Tononi G, Kötter R. The human connectome: a structural description of the human brain. PLoS computational biology. 2005;1(4):e42.
20. Sporns O, Chialvo DR, Kaiser M, Hilgetag CC. Organization, development and function of complex brain networks. Trends in cognitive sciences. 2004;8(9):418-25.
21. Gong G, He Y, Concha L, Lebel C, Gross DW, Evans AC, et al. Mapping anatomical connectivity patterns of human cerebral cortex using in vivo diffusion tensor imaging tractography. Cereb Cortex. 2009;19(3):524-36.
22. Smith RE, Tournier J-D, Calamante F, Connelly A. Anatomically-constrained tractography: improved diffusion MRI streamlines tractography through effective use of anatomical information. Neuroimage. 2012;62(3):1924-38.
23. Mahesh B. Machine learning algorithms-a review. International Journal of Science and Research (IJSR)[Internet]. 2020;9(1):381-6.
24. El Naqa I, Murphy MJ. What Is Machine Learning? In: El Naqa I, Li R, Murphy MJ, editors. Machine Learning in Radiation Oncology: Theory and Applications. Cham: Springer International Publishing; 2015. p. 3-11.
25. LeCun Y, Bengio Y, Hinton G. Deep learning. Nature. 2015;521(7553):436-44.
26. Lundervold AS, Lundervold A. An overview of deep learning in medical imaging focusing on MRI. Zeitschrift fuer medizinische Physik. 2019;29(2):102-27.
27. Yamashita R, Nishio M, Do RKG, Togashi K. Convolutional neural networks: an overview and application in radiology. Insights into Imaging. 2018;9(4):611-29.
28. Chen M, Li H, Fan H, Dillman JR, Wang H, Altaye M, et al. ConCeptCNN: A novel multi-filter convolutional neural network for the prediction of neurodevelopmental disorders using brain connectome. Medical physics. 2022;49(5):3171-84.
29. Möller C, Pijnenburg YA, van der Flier WM, Versteeg A, Tijms B, de Munck JC, et al. Alzheimer disease and behavioral variant frontotemporal dementia: automatic classification based on cortical atrophy for single-subject diagnosis. Radiology. 2016;279(3):838-48.
30. Kim JP, Kim J, Park YH, Park SB, San Lee J, Yoo S, et al. Machine learning based hierarchical classification of frontotemporal dementia and Alzheimer's disease. NeuroImage: Clinical. 2019;23:101811.
31. Bron EE, Smits M, Papma JM, Steketee RM, Meijboom R, De Groot M, et al. Multiparametric computer-aided differential diagnosis of Alzheimer′s disease and frontotemporal dementia using structural and advanced MRI. European radiology. 2017;27(8):3372-82.
32. Bouts M, Möller C, Hafkemeijer A, van Swieten JC, Dopper E, van der Flier WM, et al. Single Subject Classification of Alzheimer's Disease and

Behavioral Variant Frontotemporal Dementia Using Anatomical, Diffusion Tensor, and Resting-State Functional Magnetic Resonance Imaging. J Alzheimers Dis. 2018;62(4):1827-39.
33. Ma D, Lu D, Popuri K, Wang L, Beg MF, Initiative AsDN. Differential diagnosis of frontotemporal dementia, alzheimer's disease, and normal aging using a multi-scale multi-type feature generative adversarial deep neural network on structural magnetic resonance images. Frontiers in neuroscience. 2020;14:853.
34. Hu J, Qing Z, Liu R, Zhang X, Lv P, Wang M, et al. Deep Learning-Based Classification and Voxel-Based Visualization of Frontotemporal Dementia and Alzheimer's Disease. Front Neurosci. 2020;14:626154.
35. Neuroimaging Institute of Frontotemporal Degeneration (NIFD) 2010 [Available from: https://memory.ucsf.edu/research-trials/research/allftd.
36. Alzheimer's Disease Neuroimaging Initiative (ADNI) 2004 [Available from: https://adni.loni.usc.edu/.
37. FreeSurfer [Available from: https://surfer.nmr.mgh.harvard.edu/.
38. Klein A, Tourville J. 101 labeled brain images and a consistent human cortical labeling protocol. Front Neurosci. 2012;6:171.
39. MRtrix3 [Available from: https://www.mrtrix.org/.
40. Tournier JD, Calamante F, Connelly A. Determination of the appropriate b value and number of gradient directions for high-angular-resolution diffusion-weighted imaging. NMR Biomed. 2013;26(12):1775-86.
41. Tournier JD, Calamante F, Connelly A. Robust determination of the fibre orientation distribution in diffusion MRI: non-negativity constrained super-resolved spherical deconvolution. Neuroimage. 2007;35(4):1459-72.
42. Smith RE, Tournier J-D, Calamante F, Connelly A. The effects of SIFT on the reproducibility and biological accuracy of the structural connectome. Neuroimage. 2015;104:253-65.
43. Fornito A, Zalesky A, Bullmore E. Fundamentals of brain network analysis: Academic press; 2016.